PHYSICAL REVIEW B **90**, 180102(R) (2014)

Interplay between pressure and local symmetry in $(Pb_{1-3/2x}La_x)(Zr_{60}Ti_{40})O_3$: Emergence of a relaxor state

Y. Nahas, S. Prokhorenko, and I. Kornev

Laboratoire Structures, Propriétés et Modélisation des Solides, CNRS-UMR8580, Ecole Centrale Paris, 92290 Châtenay-Malabry, France

(Received 22 November 2013; revised manuscript received 2 September 2014; published 14 November 2014)

This study aims at inquiring into the role of hydrostatic pressure in driving the relaxor behavior within a local-symmetry-based approach to relaxor ferroelectrics. Results reveal the occurrence of a pressure-induced ferroelectric-to-relaxor crossover, clearly reflected in the experiment-matching temperature-pressure phase diagram of lanthanum-modified lead zirconate titanate. Relaxor behavior is found to occur under pressure and upon cooling due to the nucleation of local order within fractal regions, as an incipient state towards percolating ferroelectric order. Further analysis of the geometrical features of ordering process points to a manifest nontrivial disruption of the balance between competing interactions under the conjugated effects of pressure and local-symmetry constraints.

DOI: 10.1103/PhysRevB.90.180102 PACS number(s): 77.80.Jk, 77.80.B−, 77.84.Cg

In the field of ferroelectricity, relaxor ferroelectrics (or relaxors) have gained widespread interest in view of their prominent physical properties primarily emanating from disorder in their composition, such as a diffuse phase transition and dielectric relaxation [1–6]. Fundamental investigations of the effects of disorder in relaxors have mainly led to two approaches, one involving random bonds [7], the other resorting to random fields [8] and to a synthesis of these two conceptual schemes within the spherical random-bond random-field model [9]. However, in spite of numerous formulations, the microscopic origin of the relaxor behavior remains a matter of debate. Beyond the attempts of casting the relaxor behavior within formal models, hydrostatic pressure has been advocated as a suitable probe of the interatomic interactions and thus of the mechanisms underlying the relaxor behavior [10]. Specifically, pressure was shown to induce a ferroelectric-to-relaxor crossover in lanthanum-modified lead zirconate titanate (PLZT), ultimately precluding the ferroelectric transition. The mechanism of this crossover from long- to short-ranged order was attributed to a pressure-induced decrease in the correlation length that governs interactions among polar nanoregions [10]. However, it is worthwhile emphasizing that although the existence of polar regions seems doubtless to many, the mechanisms of their formation and thus their nature itself are not conclusively understood [11].

One of the major challenges in the analysis and understanding of relaxors thus resides in deciphering local properties with respect to the averaged global ones in order to characterize the pressure dependency of local order, its structure, and morphology.

Recently we have conjectured that disorder in relaxor ferroelectrics can be accounted for by means of supplemental local symmetries [12], thereby involving a gauge field [13]. Such a local-symmetry conjecture for relaxor ferroelectrics has been put forward heuristically, and developed within the first-principles-derived effective Hamiltonian scheme [14,15]. This theoretical framework has then been applied to a $(Pb_{1-3/2x}La_x)(Zr_{60}Ti_{40})O_3$ (or PLZT x/60/40) solid solution. In the noncanonical PLZT x/60/40 relaxor characterized by a diffuse relaxor-to-ferroelectric phase transition at $T_C < T_m$ [3], relaxor behavior becomes discernible for $x > 5\%$ [2,6,16]. For a composition $x = 5\%$ of La^{3+} disorder, the system is thus on the verge of the relaxor behavior and hence constitutes a good candidate for looking into the physics of the pressure-induced ferroelectric-to-relaxor crossover.

In this Rapid Communication, we investigate the mechanism underlying the pressure-induced ferroelectric-to-relaxor crossover within a local-symmetry-based approach [12]. We leverage on the considerable, but often unacknowledged, ability of local symmetry to encode local features and show how an explicit account of such an extended symmetry can effectively bridge pressure-induced local features and macroscopical properties. Analysis of the evolution with pressure of polarization, specific heat, and dielectric response points to a pressure-induced ferroelectric-to-relaxor crossover in the PLZT 5/60/40 system and yields its temperature-pressure phase diagram. An assessment of the ordering process reveals the dual effect of pressure in reducing the correlation length of polar fluctuations on one hand and enhancing the correlation length of the gauge field fluctuations on the other. The pressure-induced disruption of the balance between competing interactions thus involves a nontrivial interplay between pressure and local symmetry. This interplay unveils the effect of pressure in entailing local order and inducing the relaxor state. Finally, we discuss geometrical aspects of local order, emphasizing the role of symmetries in constraining its fractal morphology.

Practically, Monte Carlo simulations were performed using the first-principles-derived effective Hamiltonian combined with the aforementioned local-symmetry conjecture which accounts for substitutional disorder by means of a partially quenched gauge field. The total energy E_{tot} incorporates a gauge field $\{U_{ij}\}$, in addition to ferroelectric and elastic degrees of freedom, and accounts for pressure via the standard pressure-volume term PV:

$$E_{\text{tot}} = E_{\text{FE}}(\{\mathbf{u}_i\},\{\eta\}) + E_{\text{G}}(\{U_{ij}\}) + E_{\text{FE-G}}(\{\mathbf{u}_i\},\{U_{ij}\}) + PV. \quad (1)$$

Details about the implementation modalities are provided in the Supplemental Material [17] and involve the quotation of Refs. [2,12–16,18–28].

Figure 1 shows the effect of pressure on the temperature evolution of the norm of the local modes, $|\langle\mathbf{u}\rangle| = (\langle u_x\rangle^2 +$

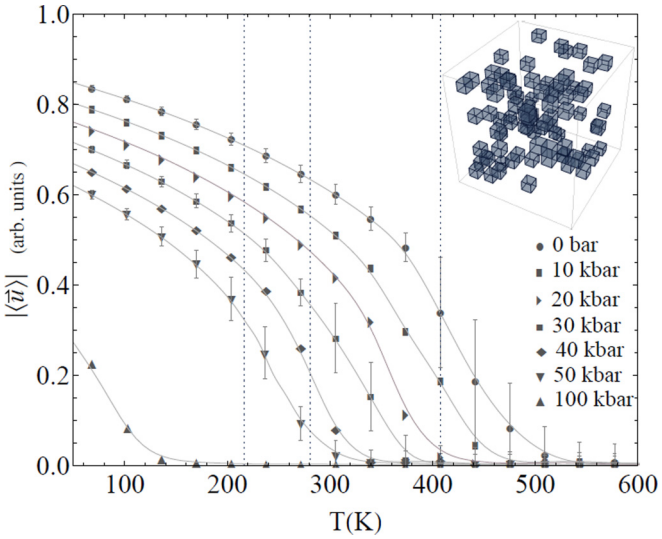

FIG. 1. (Color online) Influence of pressure on the temperature evolution of $|\langle \mathbf{u} \rangle|$ in a PLZT 5/60/40 system. Solid lines are guides to the eye. Error bars are provided for 0 bar, 30 kbar, and 50 kbar. The calculated transition temperature T_C is indicated by a dotted vertical line for each of these pressures and corresponds to the maximum of the specific heat. The inset depicts the distribution of quenched cubes (La^{3+}-containing) unit cells inside the 12^3 supercell for PLZT 5/60/40.

$\langle u_y \rangle^2 + \langle u_z \rangle^2)^{1/2}$, where $(\langle u_x \rangle, \langle u_y \rangle, \langle u_z \rangle)$ are the Cartesian components of $\langle \mathbf{u} \rangle$, and where $\langle\,\rangle$ denotes the statistical average. This effect is investigated in the range $0 \leqslant P \leqslant 100$ kbar for the same realization of disorder, i.e., the same spatial distribution of quenched La^{3+}-mimicking unit cells in the supercell (inset of Fig. 1). Increasing pressure is known to destabilize the ferroelectric phase by depressing T_C and lowering the magnitude of the polarization at low temperatures. Both of these features are indeed seen in Fig. 1, where the onset of a ferroelectric phase is ultimately precluded under high enough pressures (∼100 kbar). Moreover, it is found that whereas the subsisting tails of polarization reduce to zero within the error bars above T_C for low pressures, they retain a substantial nonvanishing value for higher pressures. These regions with polarization departing from zero above the low-temperature phase originate from finite-size scaling effects for low pressures. For higher pressures, they seem considerably less affected by finite-size effects and, as it will be later discussed, can be ascribed to the nucleation of local order in the paraelectric phase, thereby pointing to a pressure-induced ferroelectric-to-relaxor crossover.

The disordering effect of the partially quenched gauge field on the dipoles pattern is examined in Fig. 2 which depicts the integral curves [29] associated to the dipole moments field in a (x,y) plane of a 12^3 PLZT 5/60/40 supercell. For the same disorder realization (inset of Fig. 1), increasing pressure has a substantial disordering effect in that it gradually engenders local deviations from the low pressure quasiordered configuration. This is illustrated by the dark areas in Fig. 2, whose bending is all the more pronounced under increasing pressure.

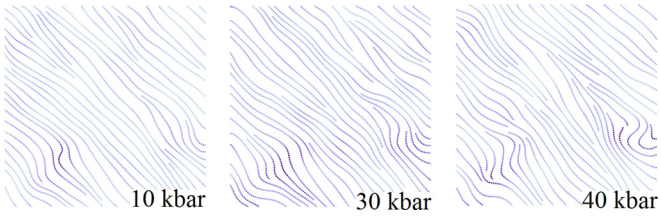

FIG. 2. (Color online) Integral curves of the local dipole moments within a given (x,y) plane for PLZT 5/60/40 at $T = 34$ K under 10, 30, and 40 kbar for the same realization of disorder. Dark areas show enhanced deviation from perfect ordering under increasing pressure.

We now turn to the analysis of the influence of pressure on the specific heat and the inverse susceptibility. The temperature at which the specific heat peaks is used for the determination of T_C while that at which the dielectric response peaks corresponds to T_m. Whereas in PZT 60/40 and PLZT 5/60/40 under 0 bar, T_C and T_m coincide, it is no longer the case for PLZT 5/60/40 under pressure for which $T_C < T_m$. We find that T_C and T_m feature a linear shift towards lower temperatures with increasing pressure. These characteristic temperatures are collected in Fig. 3, which provides the temperature-pressure phase diagram of PLZT 5/60/40. The shifts of T_C and T_m with pressure are characterized by similar slopes, namely, linear fits of the data yield $dT_C/dP = -4.85$ K/kbar and $dT_m/dP = -4.66$ K/kbar. Both the slopes and the investigated pressure range are in excellent agreement with the experimental results of Samara [10,30], who reports $dT_{C,m}/dP = -5$ K/kbar for PLZT 6/65/35.

The monotonic decrease of T_C and T_m with increasing pressure points to a manifest similarity between pressure [10] and quenched disorder content [12]. The analogy between the pressure-induced ferroelectric-to-relaxor crossover and the compositionally mediated one has been ascribed to the decrease of the correlation length for local mode fluctuations ξ_{lm} in both cases [10]. The application of pressure is thus expected to reduce ξ_{lm}, as a consequence of the pressure dependence of the soft-mode frequency which controls the

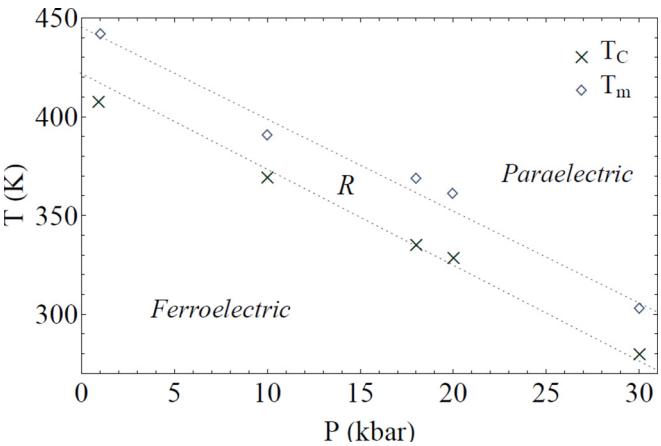

FIG. 3. (Color online) Temperature-pressure phase diagram for PLZT 5/60/40. Dotted lines delimit the relaxor region (R) and their slopes are extracted from linear fits of the T_C and T_m data.

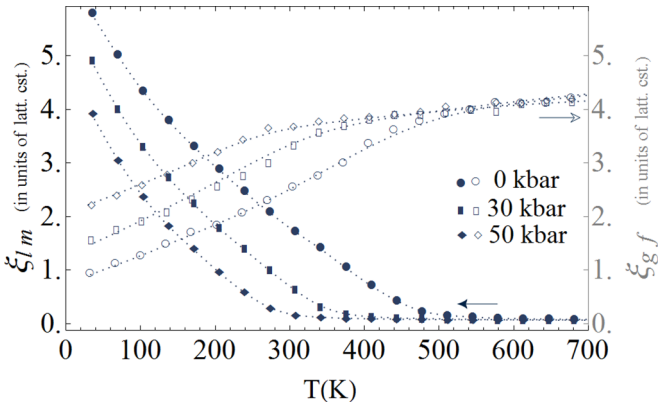

FIG. 4. (Color online) Variation of the correlation length for local modes $\xi_{\rm lm}$ (solid symbols) and gauge field $\xi_{\rm gf}$ (open symbols) fluctuations for PLZT 5/60/40 showing the influence of pressure. Dotted lines are guides to the eye.

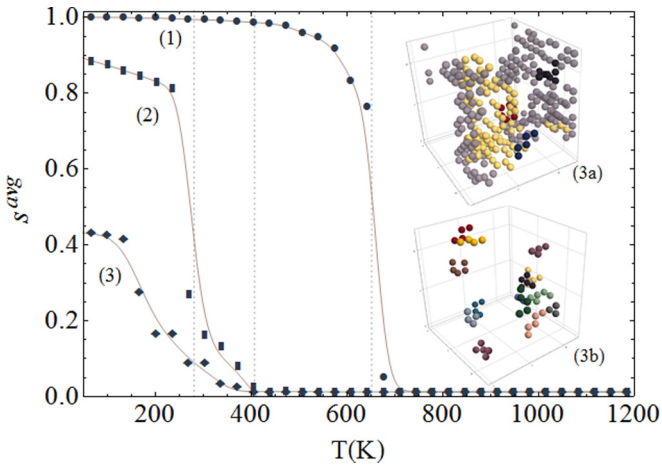

FIG. 5. (Color online) Temperature dependence of the average size of clusters $s^{\rm avg}$ for PZT 60/40 under 0 bar (1) and PLZT 5/60/40 under 0 bar (2) and 30 kbar (3). Solid lines are guides to the eye and dotted vertical lines indicate the position of T_C. The insets show the spatial distribution of the biggest clusters as obtained for PLZT 5/60/40 under 30 kbar at $T_C = 281$ K (3a), and above T_C at $T = 374$ K (3b).

polarizability of the system [2,10]. We find that pressure indeed induces a nonlinear decrease of the disconnected correlation length of the local modes in a system with fixed composition (Fig. 4), very much akin to its decrease with increasing lanthanum content [12].

To gain further insight into the ordering process of the system, we carried out the computation of the correlation length for the gauge field [31], $\xi_{\rm gf}$. In this case, $\xi_{\rm gf}$ is obtained from the plaquette-plaquette correlation function [32]. Figure 4 clearly indicates an increase of the correlation length associated to the gauge field $\xi_{\rm gf}$ when subjected to pressure. Since the partially quenched gauge field mediates disorder, this result can be understood complementarily to that pertaining to the polar fluctuations and sheds light on the origin of the effect depicted in Fig. 2. Specifically, in view of the pressure-induced reduction of $\xi_{\rm lm}$ and the coupling of the gauge variables to the dipole moments via the short-range interaction [12], pressure indirectly affects the gauge field and effectively renormalizes the self-coupling parameter k downward, yielding a strengthened gauge-mediated disorder. This is reflected in the increase of the ratio of the gauge field self-energy per spatial direction to the total energy. We find, for instance, that this ratio evolves from 5% to 21% for $T = 34$ K, under increasing pressure from 10 to 40 kbar. This comparison points to an increase of the number of thermally frustrated plaquettes $U_\square = U_{ij}U_{jk}U_{kl}U_{li}$, whose nonidentity link matrices result in unpolarized distorted regions (Fig. 2). Pressure thus impacts the relative strengths of competing interactions and reduces the stability of the ferroelectric phase. Whereas the pressure-monitored interplay between the gauge and dipolar fields results in a polarization drop at low T (Fig. 1), at higher temperatures it entails the nucleation of local order, as we will now discuss.

To achieve this purpose, we adopt a local probe allowing the investigation of local order, its morphology, and its temperature evolution under pressure. Figure 5 provides the influence of pressure on the average cluster size $s^{\rm avg}$, calculated from the ratio of the average number of local modes within clusters to the total number of local modes in the supercell 12^3, for PZT 60/40 under 0 bar and for PLZT 5/60/40 under 0 bar and 30 kbar. While $s^{\rm avg}$ drops down to negligible values above T_C in the case of PZT 60/40 and PLZT 5/60/40 under 0 bar, the existence of polar clusters in the paraelectric phase is clearly evidenced by the persisting tail above T_C for PLZT 5/60/40 under 30 kbar.

Another accessible quantity is the strength of the percolating cluster [33] that is calculated from the ratio of the number of local modes comprised within an infinite percolating cluster to the total number of local modes in the supercell. We find that the percolating signature of the phase transition into the ferroelectric phase is preserved under pressure since percolating clusters are systematically found to occur at T_C for each of PZT 60/40 under 0 bar and PLZT 5/60/40 under 0 bar and 30 kbar [inset (3a) of Fig. 5]. Accordingly, the emergence of local order above T_C in the latter system [inset (3b) of Fig. 5] characterizes the pressure-induced relaxor state as an incipient state towards percolating ferroelectric order [34]. Within our model, and in contrast to some others [9,35], polar regions are free to appear rather than constrained to exist as they are not taken to be preexisting entities but rather found to spontaneously emerge as a result of the gauge field relaxation energetics. Upon cooling, we observe a slow increase of both the number and the (relatively small) average size of clusters (containing several dipole moments) in PLZT 5/60/40 under 30 kbar. In this incipient state towards ferroelectricity [34], the system may be described as superparaelectric with weakly interacting randomly oriented polar clusters in stable equilibrium. Upon further decreasing T and approaching T_C, the rapidly growing correlation length of the local modes in PLZT 5/60/40 under 30 kbar (Fig. 4) indicates a steep increase in the size of the polar regions which merge into ultimately percolating clusters [inset (3a) of Fig. 5]. Finally, the enhanced long-range dipole-dipole interactions near the phase instability result in a cooperative ferroelectric phase below T_C.

For T just above the T_C of the PLZT 5/60/40 system under 30 kbar, we find that the total energy is comparable to that obtained for the system under 40 kbar at the same temperature. While at this temperature local probing indicates the existence of local order under 30 kbar (Fig. 5), no local-symmetry deviations at this same temperature under 40 kbar are found. Next, comparing the self-energy of the gauge field E_G under these pressures yields an energy drop for the system under 30 kbar. Given that $E_G(\{U_{ij}\}) = k\sum_{\square}(1 - \frac{1}{3}\mathrm{Tr}[U_{\square}])$, the drop indicates an increase in the number of plaquettes $U_{\square}$ that are unfrustrated and thus that locally allow collinear orientations of local modes. Further checking the spatial occurrence of these unfrustrated plaquettes, we find them subtending the obtained locally ordered regions. This energy-based consideration is thus confirmed by local probing and indicates that local order is subtended by the energetics of the gauge field. The local-symmetry constraints to which the system is subjected are therefore accountable for both the appearance of local order above T_C and the weakening of the low-temperature ferroelectric phase. The application of pressure modifies the balance of interactions and reveals that the interplay between the gauge field and the dipolar field is nontrivial. In the limit where $T \to 0$ and under the effect of pressure, quenched disorder gains influence. This effect is visualized by the spreading distortions in Fig. 2, and captured by the enhancement of ξ_{gf}, as shown in Fig. 4. Just above T_C, the gauge field locally minimizes its self-energy by featuring unfrustrated plaquettes favoring collinear dipolar configurations. With this respect, polar regions can be seen as carrying a negative volume contribution to the energy that is to be counterbalanced by a positive interface contribution, analogously to the droplet argument in frustrated spin systems [36]. Consequently, the interfaces of the polar regions can be regarded as the subspaces which encode local paraelectricity, in contrast to their volumes whose contribution to paraelectricity is only statistical. In what follows we show that above T_C, the pressure-induced local order turns out to be determined by the optimization of its surface-to-volume ratio.

An important feature of these polar regions is their structure. In order to assess the morphology of the local order, we carried out a study of the fractal dimension d_H using the box-counting method [37]. For "loose" structures, d_H is different from the topological dimension of the physical space in that it measures the deviation from compactness. We found that $d_H \sim 2.6$ in the case of PLZT 5/60/40 under 30 kbar just above T_C, thereby corroborating experimental findings [34,38] and contrasting with models within which polar nanoregions are described as compact [9], spherical entities [39], or per default assumed to be as such [40]. This result indicates that local order has developed in the paraelectric phase under the influence of pressure, and that it is comprised within clusters with rugged boundaries. This morphology most likely fulfills the requirement of a sufficiently high interface contribution so as to overcome the negative volume contribution to the energy. Furthermore, quenched disorder being randomly positioned in the lattice acts as a natural obstacle to the isotropic growth of local order. These observations indicate that the nucleation of local order within fractal morphologies most likely emanates from a surface-to-volume ratio optimization.

In summary, the application of hydrostatic pressure within a local-symmetry-based approach is shown to monotonically weaken the ferroelectric phase while gradually strengthening the emergent relaxor state. The obtained findings unravel the primary role of local symmetry in the mechanism underlying the pressure-induced ferroelectric-to-relaxor crossover. At low temperature and under the effect of pressure, quenched disorder enhances its influence by expanding its frustration network, thereby constraining dipole moments to locally adopt paraelectric configurations. At higher temperatures, regions relatively devoid of quenched disorder remain sheltered from this disordering influence, readily becoming the locus for local order found to be confined to within fractal clusters.

This work is supported by ERA.NetRUS Grant No. STProjects-133.

[1] G. A. Smolenskii and A. I. Agranovskaya, Sov. Phys. Solid State **1**, 1429 (1960).
[2] G. A. Samara, Solid State Phys. **56**, 239 (2001).
[3] A. A. Bokov and Z. G. Ye, J. Mater. Sci. **41**, 31 (2006).
[4] W. Kleeman, J. Adv. Dielectr. **02**, 1241001 (2012).
[5] A. R. Akbarzadeh, S. Prosandeev, E. J. Walter, A. Al-Barakaty, and L. Bellaiche, Phys. Rev. Lett. **108**, 257601 (2012).
[6] G. H. Haertling, J. Am. Ceram. Soc. **54**, 303 (1971); Ferroelectrics **75**, 25 (1987).
[7] D. Viehland, M. Wuttig, and L. E. Cross, Ferroelectrics **120**, 71 (1991).
[8] V. Westphal, W. Kleemann, and M. D. Glinchuk, Phys. Rev. Lett. **68**, 847 (1992).
[9] R. Blinc, J. Dolinsek, A. Gregorovic, B. Zalar, C. Filipic, Z. Kutnjak, A. Levstik, and R. Pirc, Phys. Rev. Lett. **83**, 424 (1999); R. Blinc, V. Bobnar, and R. Pirc, Phys. Rev. B **64**, 132103 (2001).
[10] G. A. Samara, Phys. Rev. Lett. **77**, 314 (1996); J. Appl. Phys. **84**, 2538 (1998).
[11] J. Hlinka, J. Adv. Dielectr. **2**, 1241006 (2012).
[12] Y. Nahas and I. Kornev, Europhys. Lett. **103**, 37013 (2013).
[13] M. Creutz, L. Jacobs, and C. Rebbi, Phys. Rep. **95**, 201 (1983).
[14] W. Zhong, D. Vanderbilt, and K. M. Rabe, Phys. Rev. Lett. **73**, 1861 (1994).
[15] L. Bellaiche, A. Garcia, and D. Vanderbilt, Ferroelectrics **266**, 41 (2002).
[16] D. Viehland, X. Dai, J. Li, and Z. Xu, J. Appl. Phys. **84**, 458 (1998).
[17] See Supplemental Material at http://link.aps.org/supplemental/10.1103/PhysRevB.90.180102 for methodological details.
[18] S. B. Vakhrushev, B. E. Kvyatkovsky, A. A. Naberezhnov, N. M. Okuneva, and B. P. Toperverg, Ferroelectrics **90**, 173 (1989).
[19] G. Xu, G. Shirane, J. R. D. Copley, and P. M. Gehring, Phys. Rev. B **69**, 064112 (2004).

[20] T. Egami, Ferroelectrics **267**, 101 (2002).
[21] N. deMathan, E. Husson, G. Calvarin, J. R. Gavarri, A. W. Hewat, and A. Morell, J. Phys.: Condens. Matter **3**, 8159 (1991).
[22] P. Bonneau, P. Gamier, E. Husson, and A. Morell, Mater. Res. Bull. **24**, 201 (1989).
[23] A. Kadic and D. G. B. Edelen, *A Gauge Theory of Dislocations and Disclinations* (Springer, Berlin, 1983).
[24] M. K. Kharrasov, I. R. Kyzyrgulov, and A. T. Khusainov, Dokl. Phys. **53**, 360 (2008).
[25] G. Toulouse, Commun. Phys. **2**, 115 (1977).
[26] I. E. Dzyaloshinskii and G. E. Volovik, J. Phys. (Paris) **39**, 693 (1978).
[27] M. O. Katanaev and I. V. Volovich, Ann. Phys. **216**, 1 (1992).
[28] P. Goldbart, O. Martin, and E. Fradkin, Phys. Rev. B **34**, 301 (1986).
[29] V. I. Arnold, *Ordinary Differential Equations* (MIT Press, Cambridge, MA, 1973).
[30] G. A. Samara and E. L. Venturini, Phase Transitions **79**, 21 (2006).
[31] W. Janke and K. Nather, Phys. Rev. B **48**, 7419 (1993).
[32] G. Bhanot and C. Rebbi, Nucl. Phys. B **180**, 469 (1981).
[33] D. Stauffer and A. Aharony, *Introduction to Percolation Theory*, 2nd revised ed. (Taylor and Francis, London, 2003).
[34] A. Koreeda, H. Taniguchi, S. Saikan, and M. Itoh, Phys. Rev. Lett. **109**, 197601 (2012).
[35] L. E. Cross, Ferroelectrics **76**, 241 (1987); **151**, 305 (1994).
[36] D. S. Fisher and D. A. Huse, Phys. Rev. Lett. **56**, 1601 (1986).
[37] S. Buczkowski, P. Hildgen, and L. Cartilier, Physica A **252**, 23 (1998).
[38] V. Ya. Shur, G. G. Lomakin, V. P. Kuminov, D. V. Pelegov, S. S. Beloglazov, S. V. Slovikovski, and I. L. Sorkin, Phys. Solid State **41**, 453 (1999).
[39] S. Tinte, B. P. Burton, E. Cockayne, and U. V. Waghmare, Phys. Rev. Lett. **97**, 137601 (2006).
[40] B. E. Vugmeister, Phys. Rev. B **73**, 174117 (2006).